Research on Engineering Structures & Materials
www.jresm.org
Research Group

Research Article

Computational modeling and process parameter optimization of straw fiber winding and weaving in sustainable packaging design

Lili Mo [1,2,a]; Velan Kunjuraman [*,1,b], Novel Lyndon [1,c], Yantu Ma [3,d] , Liang Meng [4,e]

[1]*Centre for Research in Development, Social and Environment, Faculty of Social Sciences and Humanities, University Kebangsaan Malaysia, Selangor, Malaysia*
[2]*Faculty of Art and Media, Nanning College of Technology, Nanning, China*
[3]*Center for Software Technology and Management, Faculty of Information Science & Technology University Kebangsaan Malaysia, Selangor, Malaysia*
[4]*School of Art and Design, Guilin Tourism University, Guilin, 541006, China*

Article Info

Article History:

Received 11 Jun 2026

Accepted 05 Sep 2026

Keywords:

Straw fiber composites;
Sustainable packaging;
Filament winding;
Computational modeling;
Process parameter optimization;
Multi-objective optimization

Abstract

The transition toward a low-carbon and circular economy has increased the demand for sustainable alternatives to petroleum-based packaging materials. Natural fiber reinforced polymer composites (NFRPCs) have gained attention due to their low density, high specific strength, renewability, and biodegradability. However, manufacturing complex three-dimensional packaging structures remains challenging because of fiber heterogeneity, weak fiber–matrix adhesion, and nonlinear thermo-mechanical interactions during processing. This study proposes an integrated framework combining multi-scale mechanics modeling, experimental validation, and multidisciplinary design optimization (MDO) for the development of high-performance green packaging components. Mechanical behavior was predicted using the rule of mixtures and Halpin–Tsai models, while Darcy's law and heat transfer equations were employed to analyze resin impregnation and thermal evolution. A real-time filament winding and weaving platform was established to obtain experimental data. Box–Behnken design (BBD) and Response Surface Method (RDM) were used to evaluate the effects of heating temperature, winding tension, winding speed, and roller pressure on tensile strength, porosity, and energy consumption. The Non-dominated Sorting Genetic Algorithm (NSGA-II) was then applied to identify Pareto-optimal process parameters. Experimental validation confirmed the accuracy of the optimized results, the results obtained using the optimized process show that there is a 10.46% improvement in tensile strength, 37.40% decrease in porosity, and 1.00% decrease in specific energy consumption as compared to the original process, showing the practical value of the suggested NSGA-II optimization approach, providing a reliable approach for designing sustainable packaging materials from agricultural waste.

© 2026 MIM Research Group. All rights reserved.

1. Introduction

With the acceleration of global industrialization and the rapid expansion of the consumer market, the excessive use and disposal of traditional petroleum-based plastic packaging have triggered a catastrophic environmental crisis. According to relevant environmental assessment reports, if no effective intervention measures are taken, by 2040, the pollution caused by plastic packaging will

*Corresponding author: velan@ukm.edu.my
[a]orcid.org/0009-0008-4793-1589; [b]orcid.org/0000-0002-5616-4712; [c]orcid.org/0000-0001-5049-8247;
[d]orcid.org/0009-0008-8361-7896; [e]orcid.org/0009-0002-3133-1278
DOI: http://dx.doi.org/10.17515/resm2026-1742ma0611rs

increase by more than double, becoming the largest single source of land and marine microplastic pollution in the world [1]. Against this backdrop, the development of alternative materials with high mechanical properties and friendly to the environment has become a major strategic demand in the fields of packaging engineering and materials science. Natural fiber reinforced bio composites, with their unique advantages of being renewable, having low carbon emissions, and being fully biodegradable, are gradually demonstrating great application potential in food packaging, heavy logistics cushioning components, and consumer electronic outer packaging fields [2,3].

Among various natural fiber resources, agricultural wastes such as wheat straw, rice straw, and sorghum straw not only have abundant reserves and low costs, but also their microscopic cellulose crystalline regions endow the materials with excellent specific stiffness, thermal insulation, and buffering properties [4]. For a long time, these agricultural wastes have mostly been directly burned or buried, which not only wastes valuable lignocellulosic resources but also exacerbates greenhouse gas emissions and regional air pollution [3]. Agricultural activities produce more than 4 billion tonnes of crop residues every year worldwide, wheat straw being one of the most abundant renewable lignocellulosic resources [2,3]. However, only a small fraction of it is being used effectively, with the rest being burned or dumped openly in the environment causing pollution and greenhouse gas emissions [3,4]. The growing trend of decreasing usage of petroleum-based packaging has led to the use of natural-fiber-based composites as environmentally friendly packaging alternatives [5,6].

In summary, straw-fiber composite packaging has high industrial value, which can effectively utilize large-scale straw resources and realize circular bioeconomy, thereby utilizing the abundant straw resources on farms to produce value-added straw products, and upgrading straw resources. Although a large number of studies have attempted to incorporate straw fibers in the form of short chips or powder into thermoplastic resins through injection molding or compression molding to manufacture flat panels [5], these traditional molding processes are difficult to meet the strict requirements of modern logistics packaging for complex three-dimensional shapes, local load customization, and high impact resistance. In contrast, continuous filament winding and three-dimensional weaving technologies can achieve precise placement of reinforcing fibers in the spatial structure, maximize the volume fraction of the fibers, and endow the structural components with excellent anisotropic mechanical properties, making them cutting-edge processes for manufacturing high-performance lightweight composite material structures [6-9].

However, in the manufacturing of complex three-dimensional packaging components, the continuous filament winding of agricultural waste (such as wheat straw fibers) and the automated three-dimensional weaving process are still constrained by the microstructural heterogeneity of the fibers, the weak interfacial adhesion, and the nonlinear coupling effect of thermal mechanical processing parameters. For instance, Mishra et al. studied the structural optimization potential of environmentally friendly composite materials based on agricultural waste (such as straw and sugarcane residue) in food storage and packaging [1,10]. Meanwhile, the parameter optimization study on the mixed fiber membrane of pineapple leaves and rice straw further demonstrated the wide applicability of agricultural waste fibers in sustainable packaging [2,11]. Firstly, unlike synthetic fibers with high consistency and extremely high thermal stability (such as carbon fibers or glass fibers), straw fibers have extremely strong natural heterogeneity. The wax layer and siliceous structure covering their surfaces severely hinder the effective infiltration of resins, resulting in weak interfacial bonding force [12]. Secondly, the thermal resistance threshold of straw fibers is relatively low (typically around 200C, where semi-cellulose and lignin undergo thermal degradation), which makes traditional in-situ curing or hot air-assisted winding process parameters no longer applicable. Even a slight deviation can lead to thermal damage to the fibers or incomplete resin impregnation, thereby generating a large number of internal pore defects [13]. Moreover, the filament winding and weaving process involves complex coupling of multiple physical fields such as heat conduction, fluid dynamics, large fiber deformation, and contact friction. The traditional "trial-and-error method" is not only costly but also difficult to reveal the nonlinear interaction mechanisms among various process parameters.

To overcome the aforementioned technical bottlenecks, it is particularly urgent to introduce the multi-disciplinary design optimization (MDO) theory into the manufacturing process of natural fiber composites. The MDO method, by integrating computational material science, systematic experimental verification, and advanced meta-heuristic algorithms, can perform global optimization on the design variables of complex systems [14]. This study established a complete physical experimental and theoretical computational optimization framework for the winding and braiding process of straw fiber/poly (lactic acid) (straw fiber/PLA) prepreg tapes. The proposed framework combines innovative engineering-material analysis with automated composite manufacturing and performance-oriented optimization for sustainable packaging structures. The core objectives of this research include three aspects: Firstly, construct a theoretical model covering micro-mechanical predictions and macro-winding kinematics, and conduct in-depth physical experiments based on the actual process platform; Secondly, use BBD AND RSM to quantify the linear and nonlinear effects of heating temperature, winding tension, roll pressing, and winding speed on the actual tensile strength, porosity, and unit energy consumption of the composite materials; Thirdly, combine the NSGA-II for multi-objective process optimization, aiming to ensure the mechanical reliability of packaging components, while maximizing manufacturing quality and minimizing energy consumption.

2. Literature Review

In the fields of natural fiber packaging material design and advanced manufacturing of composite materials, previous researchers have conducted a large amount of basic and theoretical studies. Conducting a systematic and critical analysis of these studies is helpful for accurately assessing the scientific value and innovative breakthroughs of this research.

2.1 The Evolution and Limitations of Natural Fiber Reinforced Composites in the Packaging Field

Natural plant fibers have been widely studied and utilized as reinforcing phases in composite materials due to their environmentally friendly characteristics. Previous studies provided a detailed overview of the latest advancements in plant-based natural fiber composite materials, highlighting their significant lifecycle environmental advantages in replacing glass fibers for medium and low-load structural components [3]. In the packaging application field, Srivastava and Singh evaluated the potential of bio-composite materials in reducing the carbon footprint of the packaging industry, emphasizing the importance of converting agricultural waste (such as jute, banana leaf fiber, and banana pseudo stem) into high-value packaging products [2]. Researchers conducted a series of studies on wheat straw fibers, optimizing the raw material ratio and pulping degree of straw fiber seedling pots through orthogonal experiments, and proving that high content of straw fibers can both maintain structural integrity and provide excellent degradation performance. Mosi et al. used the fused deposition modeling (FFF) technology to study the mechanical properties of 3D-printed coconut shell fiber-reinforced polypropylene composites, finding that adding an appropriate number of natural fibers can effectively improve the bending modulus and compression modulus of the matrix [15].

However, the current literature on the research of natural fiber packaging materials mostly focuses on the random dispersion mixing of chopped fibers or simple planar hot-pressing molding. The stress transfer efficiency within such materials is low, and they cannot withstand the multi-directional dynamic impacts in complex logistics environments. Besides traditional packaging applications, the mechanical reinforcement mechanism of wheat straw fibers in soil-based and cement-based composite material systems has also been widely verified. The microscopic interface interactions provide important references for the research on polymer-based composite materials [3,16]. Moreover, the feasibility of using rice straw fibers to manufacture fully biodegradable agricultural seedling pots and mats has been confirmed through multi-factor regression orthogonal experiments [17]. However, the research on constructing high-capacity three-dimensional topological packaging structures using continuous wheat straw fibers or high-twist wheat straw yarns through winding and weaving techniques is still in its infancy and faces many technical challenges.

2.2 Mechanical Modeling Techniques for Composite Fabrication and Winding Processes

The involvement of material constitutive theories and computational mechanics has significantly advanced the theoretical development of composite material manufacturing processes. For three-dimensional weaving and winding structures, Gil Pérez et al. proposed a collaborative design framework based on coreless filament winding (CFW), by abstracting fiber bundles as spatial line segment elements, achieving rapid mechanical assessment and shape optimization for complex topological structures [18]. Doersam et al. developed a textile composite structure for tubular tissue scaffolds and used theoretical models to evaluate the control mechanisms of different weaving architectures (such as plain weave, twill, satin) on the macroscopic flexibility and pore distribution of the structure, demonstrating the decisive role of mesoscopic geometric forms in macroscopic performance [19]. In the field of forming dynamics of fiber winding processes, Meshram et al. established an analytical model for heat conduction during ultrasonic-assisted thermoplastic prepreg winding, successfully predicting the temperature field distribution law of the resin during curing [20].

Although the process theoretical models for synthetic fiber composites are relatively mature, directly transplanting them to natural fiber systems faces serious incompatibility issues. Natural fibers have highly irregular cross-sections, inherent pore structures, and strong moisture and heat sensitivity. Existing fluid impregnation models (such as the traditional Kozeny-Carman equation) often assume fibers as perfect incompressible cylinders, which leads to significant theoretical deviations when predicting the resin permeability of straw fibers. Therefore, it is urgently necessary to establish customized mathematical mechanical models that fully consider the microscopic morphological characteristics and interface properties of natural fibers based on physical experiments. Senk et al. used representative volume elements (RVE) to deeply explore the mechanical behavior of plant fiber-reinforced composite materials under failure limits, revealing the influence laws of mesoscopic geometric parameters on macroscopic strength [21]. In the microscopic mechanical analysis of mixed fiber composites of flax and jute, the finite element method was proven to be more accurate than traditional analytical models in predicting the stiffness synergy effect [22]. Additionally, for the large deformation of fibers in continuous winding processes, the analysis of fabric curling rate (crimp factor) based on three-dimensional finite elements also indicates that non-orthogonal trajectories have a significant impact on the weaving stability of carbon fibers or plant filaments [23]. For the nonlinear constitutive equation simulation of agricultural straw composite materials, some scholars adopted multi-scale meshing technology, successfully capturing the evolution process of internal stress concentration [24].

2.3 Multidisciplinary and Multi-Objective Optimization Strategy for Composite Material Process Parameters

The filament winding and weaving process is a typical highly nonlinear and multi-variable strongly coupled system. The RSM was used to conduct multi-response interval sensitivity analysis on the prepreg winding process, revealing the interactive influence mechanism of winding tension and heating temperature on the interlayer shear strength and porosity of the final composite material, and proving that the winding tension plays a core role in inhibiting the evolution of matrix pores [25]. Scholars evaluated the parameter optimization of carbon fiber reinforced polyamide 6 (CF/PA 6) composite materials during the molding process through systematic experiments, focusing on the profound influence of cooling rate and molding pressure on the matrix crystallization behavior and impact resistance [26]. They then discussed the restrictive relationship between heat source power and winding speed on the interface bonding quality for the laser-assisted winding process [13]. However, in practical engineering applications, the optimization of a single indicator often comes at the expense of other performances. For example, blindly increasing the heating temperature to reduce the porosity and reducing the production speed will inevitably lead to an increase in the risk of material thermal degradation and a significant increase in production energy consumption, which is contrary to the original design intention of green and sustainable packaging. To solve such multi-objective conflicts, emphasized the statistical advantages of BBD in reducing the number of experiments and constructing precise polynomial

surrogate models [27]; while other studies demonstrated the powerful ability of combining response surface models with heuristic algorithms (such as NSGA-II) to conduct global Pareto frontier optimization for complex systems in the MDO of spacecraft structures [14]. Integrating this advanced MDO optimization strategy into the experimental verification and process manufacturing of agricultural biological composite materials is an unexplored frontier area in current literature and is also the core scientific problem that this study aims to address. Ghadge et al. emphasized in a recent authoritative review on MDO of composite material structures that combining surrogate models with intelligent heuristic algorithms is the best approach to solve the high computational cost and nonlinear coupling problems [4,28]. For the physical performance prediction of textile polymer composite materials, multi-objective optimization algorithms (such as NSGA-II) have been successfully used to optimize artificial neural networks, significantly improving the design efficiency [5,29]. In the planning of winding paths for complex tubular and non-circular cross-section structures, trajectory optimization of the robot end effector based on differential evolution algorithm has achieved the optimal control of fiber placement angles [30]. It was pointed out in the research on the modification of the Halpin-Tsai empirical model that in multi-objective decision-making, an accurate mesoscopic stiffness surrogate model is the prerequisite for preventing optimization from falling into non-physical local optima [31].

3. Research Methods and Experimental Modeling

In order to precisely capture the mechanical and rheological laws of straw fibers during the winding and weaving processes in theory, and to utilize the actual test data to guide the subsequent optimization of process parameters, this study has designed a deeply integrated physical experiment and theoretical calculation framework. This framework starts from the mesoscopic scale material prediction equations and extends upwards to the kinematic control of experimental equipment, ultimately constructing a multi-objective experimental data decision model based on machine learning algorithms. To present the systematic approach of this research more clearly, Fig 1 depicts the core MDO workflow architecture relied upon in this study.

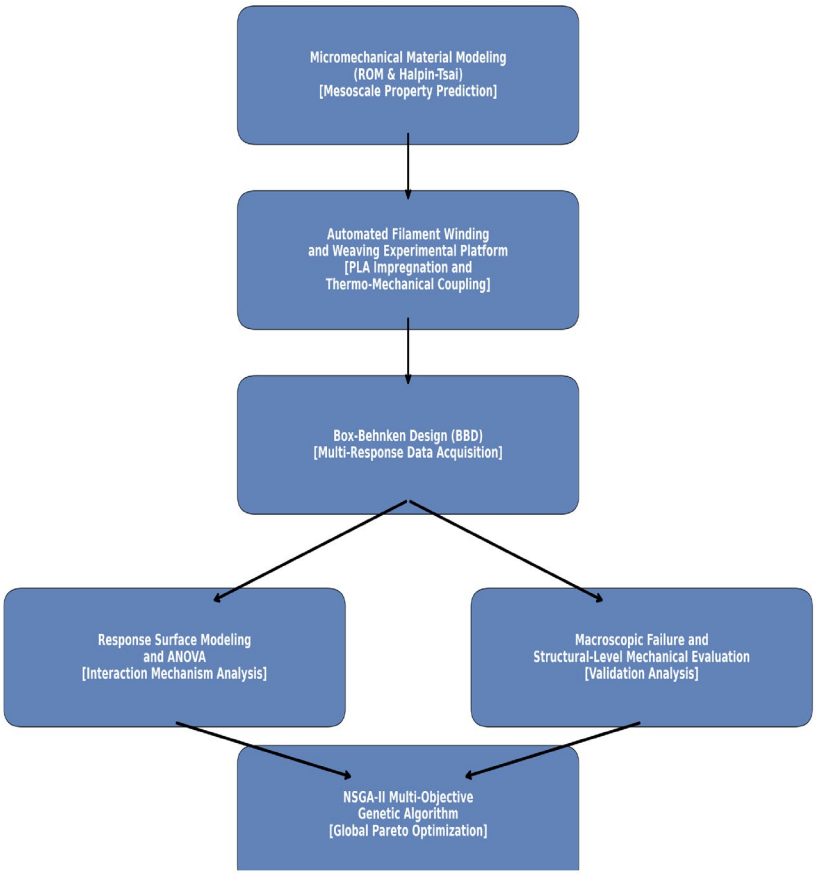


Fig. 1. Multi-disciplinary design optimization (MDO) workflow architecture

As shown in Fig. 1, the system architecture is divided into four key layers:

- Firstly, extract and predict the potential mesoscopic features.
- Secondly, conduct macroscopic winding and weaving processing based on the physical experimental platform; Then, use the RDM for data-driven modeling.
- Finally, execute the top-level global Pareto optimization through the NSGA-II algorithm.

3.1 Pre-Treatment of Straw Fibers and Modeling of Mesoscopic Mechanics Theory

The original physical state of natural wheat straw cannot directly meet the requirements of continuous fiber winding. Before the formal experiment, the raw materials of the straw underwent a standardized physical-chemical combined pre-treatment process. Following the mature schemes from relevant literature, the pre-treatment included mechanical rubbing and crushing, and a 2-hour alkaline degumming treatment at 90°C using a 5% NaOH solution. After alkali treatment, the straw fibers were washed clean with plenty of water to eliminate the alkali and dirt that remain on the surface. In order to prevent the effect of the residual chemicals on the fiber–matrix interface, the washing process was further continued till the complete neutralization. These treated fibers were then dried prior to resin impregnation to remove moisture and to provide uniform conditions for processing. Such post-treatment steps were added for the purposes of reproducibility and accurate replication of the preparation procedure for fibers. This was to effectively dissolve and remove the siliceous layer, waxy substances, and some hemicellulose on the surface, thereby significantly increasing the relative crystallinity of cellulose and improving the surface roughness [3-5,12].

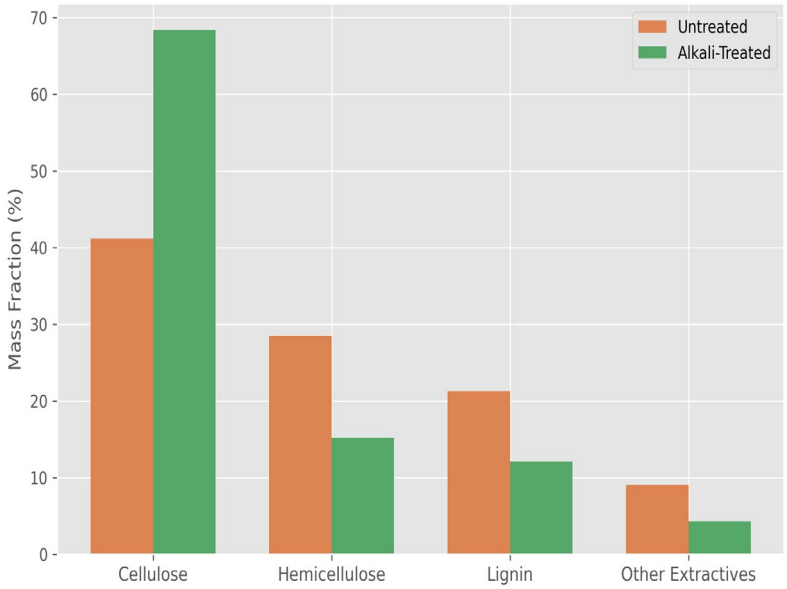


Fig. 2. The graph showing the changes in crystallinity and component composition of straw fibers before and after pretreatment

Fig. 2 visually demonstrates the impact of the chemical-physical combined pretreatment on the microscopic composition of the straw fibers. It is clearly observable that the untreated original fibers contain a high proportion of lignin and hemicellulose, which significantly reduces the thermal stability and resin wettability of the fibers. After alkali liquid delignification treatment, the components in the amorphous zone are largely removed, and the relative proportion of cellulose significantly increases, while the crystallinity is greatly enhanced, laying a structural foundation for the subsequent jump in the strength of the composite material. After combing and stretching, continuous straw fiber bundles are formed, and then they are compounded with the poly(lactic acid) (PLA) resin melt in the experimental extrusion mold to prepare continuous thermoplastic pre-impregnated strips (with a cross-sectional size of 12 mm wide and 0.5 mm thick).Before conducting macroscopic tests such as stretching, this study introduced the micro-mechanics

equations to make a benchmark prediction of the effective mesoscopic mechanical properties of the composite prepreg tape.

In the mechanics of composite materials, the most fundamental prediction tool is the rule of mixture (ROM), which can calculate the longitudinal elastic modulus E_c of the composite system under ideal conditions (1):

$$E_c = E_f V_f + E_m V_m \tag{1}$$

Among them, E_f and E_m represent the elastic modulus of the straw fibers and the PLA matrix respectively, while V_f and V_m are the corresponding volume distribution rates. However, since the straw fibers have a typical orthotropic natural structure and irregular geometric cross-section, simple ROM often overestimates the lateral and shear properties of the material. Therefore, this study further adopted the widely used Halpin-Tsai (H-T) semi-empirical model to more accurately predict the effective composite modulus M that takes into account the fiber aspect ratio and the geometric arrangement characteristics of the matrix (2):

$$M = M_m \frac{1 + \xi \eta V_f}{1 - \eta V_f} \tag{2}$$

In the model, the definition of parameter η is (3):

$$\eta = \frac{E_f - E_m}{E_f + \xi E_m} \tag{3}$$

In the formula, M represents the elastic modulus of the composite material (such as E_{11}, E_{22} or shear modulus G_{12}), M_m is the corresponding modulus of the pure PLA matrix, and ξ is a dimensionless empirical shape factor related to the fiber geometry, stacking structure, and loading direction. These theoretical calculated values provide a reliable mathematical benchmark for evaluating whether the interface impregnation in the subsequent physical experiments reaches the ideal state. The physicochemical characteristics and statistical variability of the raw straw fibers are presented in Table 1 to ensure material consistency and establish reliable input parameters for the developed straw fiber/PLA composite model. Fiber length distribution, diameter variation, moisture content, chemical composition, density and tensile properties were assessed prior to composite fabrication, to determine the quality of the fibres as reinforcement and the reproducibility of the selected natural fibres. The statistical analysis based on mean, standard deviation, minimum-maximum values and coefficient of variation proves that raw fibres contain an inherent variability and proves their suitability for the processing of composites. The cellulose contents measured and properties of the fibers are important data for understanding reinforcement ability and load transfer efficiency in the PLA matrix while the moisture content is useful for controlling voids and interfacial adhesion during manufacturing. Experimentally obtained properties of the fibers were then integrated into the mathematical model and optimization framework to enhance the accuracy of the tensile strength and porosity prediction of the optimized straw fiber/PLA composite. The mechanical properties of the straw fiber composite were estimated by the Rule of Mixtures (ROM) model and the Halpin–Tsai model, which can predict the elastic behavior of natural fiber-reinforced composites with relatively low computational complexity. In order to estimate the longitudinal elastic modulus, the ROM was used, while the Halpin–Tsai model was used to characterize the transverse elastic response taking into account the fiber reinforcement efficiency. Both models are based on the assumption of a uniform dispersion of fibers, effective fiber-matrix interface bonding and linear-elastic material behavior. The models selected offer an effective compromise between the computational efficiency and prediction accuracy of the proposed process optimization framework when compared to the Mori–Tanaka [32] and self-consistent micromechanical models [33], the Halpin–Tsai approach provides an efficient combination of computational efficiency and predictive accuracy, which makes this model well-suited for stiffness calculation and optimization of natural fiber composites. The theoretical predictions were then compared with the experimental measurements, and although they may be influenced with the non-uniform fiber orientation and interfacial imperfections, the results showed

that such models are appropriate for the evaluation of mechanical performance of the proposed straw fiber composite packaging system.

Table 1. Physicochemical characterization and variability analysis of raw straw fibers

Property	Unit	Mean ± SD	Minimum	Maximum	Coefficient of Variation (%)	Characterization Method
Fiber Length	mm	41.8 ± 5.2	32.4	52.6	12.4	Optical microscopy
Fiber Diameter	μm	186 ± 24	142	231	12.9	SEM/Image analysis
Moisture Content	%	6.4 ± 0.5	5.6	7.3	7.8	ASTM D4442
Cellulose Content	%	58.7 ± 2.3	55.2	62.4	3.9	Chemical analysis
Hemicellulose Content	%	17.8 ± 1.5	15.4	20.3	8.4	TAPPI method
Lignin Content	%	13.2 ± 1.1	11.4	15.1	8.3	Klason lignin
Ash Content	%	5.1 ± 0.4	4.5	5.8	7.8	ASTM D1102
Density	g/cm^3	1.29 ± 0.04	1.23	1.35	3.1	Pycnometer
Tensile Strength of Fiber	MPa	312 ± 28	261	356	9	Single fiber tensile test

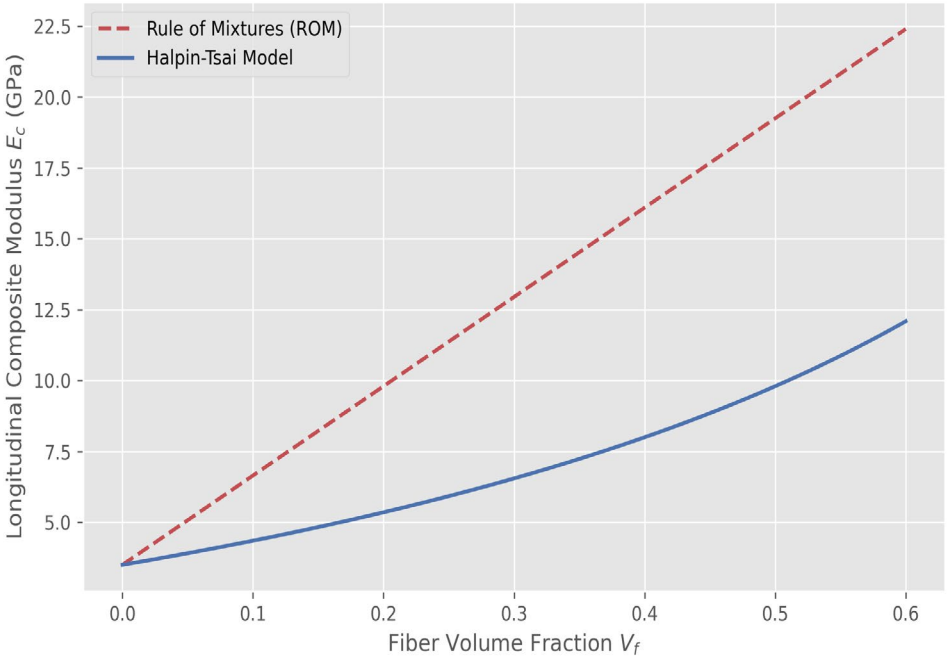


Fig. 3. Comparison of composite modulus predictions for different micro-mechanical models

As shown in the theoretical predicted evolution curve of Fig 3, the traditional ROM linear rule, due to not considering the non-ideal transfer of the microscopic cross-sectional shape and interface when the fiber volume fraction is high, leads to a significantly overestimated prediction. However, the Halpin-Tsai curve, after introducing the empirical shape factor, presents a nonlinear trend that is more in line with the actual stiffness growth of natural plant fibers. This also emphasizes the necessity of using the modified micro-mechanical model as a reference benchmark in the development of bio-based packaging composite materials. The approaches used in analysis are

systematic methods that can be used to understand material – property relationships and to make predictions about the mechanical responses of the engineered composite structure.

3.2 Physical Experiment Platform and Mathematical Control Model for Winding and Weaving Processes

The three-axis winding and weaving platform was designed to be an automatic one, in which the mathematical trajectory model was used as the manufacturing layer of the proposed integrated framework, connecting the mathematical trajectory with the experimental process-control parameters. The winding trajectory was controlled by a programmable logic controller (PLC), and the fiber-feeding and press-roller compaction operations were controlled by the PLC, while the infrared heating unit supplied local heat for impregnation of thermoplastic PLA. The winding process was carried out in the experimental range of the following parameters: the heating temperature 170–210 °C, the winding tension 20–60 N, the roller pressure 1.0–3.0 MPa and the winding speed 50–150 mm/s. The resultant winding-layer information was used in a PLC based control system to keep the fiber placement and thickness of the structure under control, and the conditions of the processes were monitored in the fabrication to ensure experimental consistency. This involved process control and monitoring and led to a clearer experimental procedure by linking the controlled manufacturing parameters to the physical processing operations, the experimental data collected and the subsequent optimization. In this way, the automation concept set up a continuous process chain between the mathematical trajectory control and the physical material deposition on the one hand, and the experimental data acquisition and multi-objective optimization of the process.

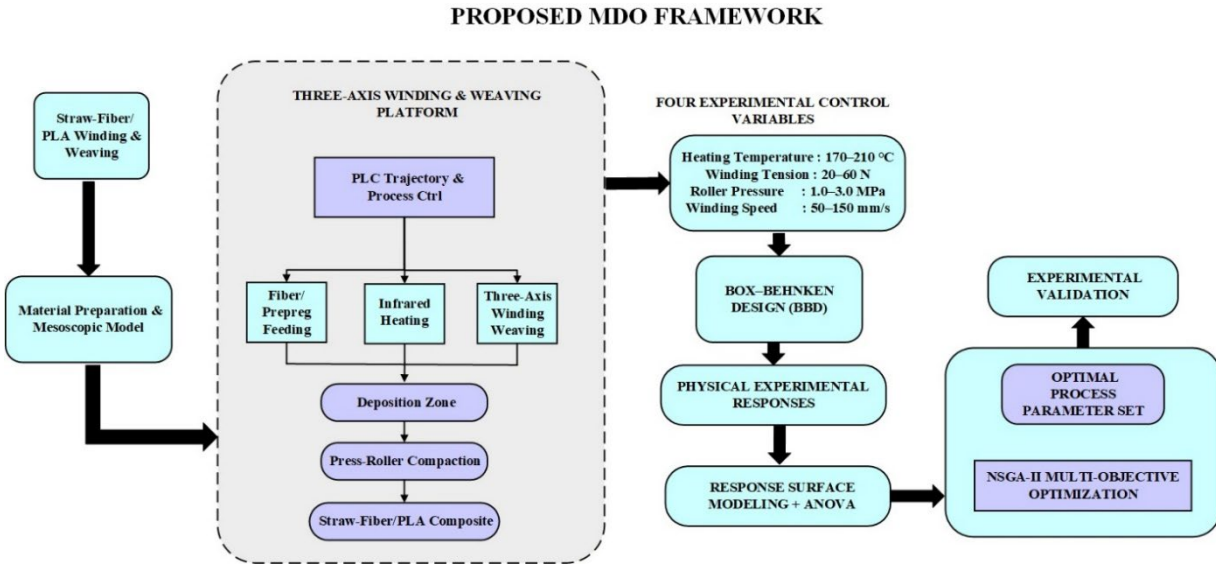


Fig. 4. Schematic representation of the automated three-axis winding and weaving platform, process-monitoring configuration, and integrated experimental optimization workflow

The proposed straw-fiber/PLA composite fabrication integrated manufacturing and optimization workflow are shown in Fig 4. The trajectory and process control system is based on the PLC, which integrates the fiber/prepreg feeding, infrared heating, winding/weaving, deposition and the press-roller compaction of the winding/weaving process. The Box–Behnken design (BBD) is used for systematic variation of process conditions, such as heating temperature, winding tension, roller pressure and winding speed. Process monitoring is integrated to the manufacturing process at the appropriate manufacturing phases to monitor the operating conditions during manufacturing. The produced samples are tested experimentally for their tensile strength, porosity and specific energy consumption. The consequent responses are then analyzed by response surface modelling and ANOVA, after which optimization of these multi-objective responses is done using NSGA-II multi-objective optimization to provide the optimal set of process parameters, finally validated in experiments.

3.2.1 Number of Wrapping Layers and Morphology Control Equation

In actual processing, in order to ensure the uniformity of the wall thickness and the target mechanical properties of the packaging cylindrical body or the buffer curved surface structure component, it is necessary to precisely control the coverage rate of the fibers and the number of wrapping layers through geometric and kinematic means. The wrapping-layer model establishes the relationship between the winding trajectory and the required layer arrangement to achieve uniform fiber distribution during composite fabrication. The governing equation was derived from the geometric properties of the winding path, and the required surface coverage. This allowed the number of winding layers to be calculated. The calculated fiber layer configuration was used to control the fiber placement sequence during the automatic winding to ensure the uniformity of the fiber layer structure and the stability of its manufacturing process in the proposed straw-fiber composite packaging system. In the platform control system, on the surface of the core mold with a cross-sectional radius of ρ, the mathematical control equation for the average number of fiber coverage layers $N_L(\rho)$ is set as (4):

$$N_L(\rho) = \frac{W_f cos\alpha \times t_w \times 2}{2 \times \pi \times \rho} \tag{4}$$

In the equation, W_f represents the actual laying width of a single pre-impregnated tape, α is the actual winding angle between the fibers and the core mold warp lines, and t_w is the coefficient of the main shaft rotation period time. This equation serves as the input source for the programmable logic controller (PLC), ensuring the consistency of the macroscopic dimensions of each experimental sample and eliminating the experimental errors caused by fluctuations in the structural thickness.

3.2.2 Resin Rheology and Impregnation Control Model

The void content (VC) is a critical defect indicator that determines the fatigue resistance and moisture-proof performance of packaging composite materials. Under the contact pressure applied by the press roller, the molten PLA resin undergoes squeeze flow within the porous straw fiber bed to expel the trapped air. The resin-infiltrating process of the straw-fiber preform was modeled with Darcy's law for anisotropic porous medium. The conventional porous flow analysis is a relationship that expresses the velocity of the resin as a function of the pressure gradient by a scalar value of permeability coefficient.

The woven straw-fiber structure, however, has directionally dependent pore structure and flow resistance, which is represented by a second order permeability tensor K that extends the scalar permeability coefficient to account for the anisotropic properties of the preform. The permeability tensor was calculated by applying the structural properties of the arrangement of the straw fibers (fiber orientation, woven structure, distribution of internal pore in the fibers), which directly affect the resistance of resin transport. The anisotropic assumption assumes that the aligned fiber network has different resin flow behaviors in various directions. Hence, the permeability tensor determines the speed of resin infiltration, uniformity of flow and quality of impregnation and can therefore be used to predict resin filling in the fabrication of the proposed straw-fiber composite packaging system with accuracy. This physical flow process conforms to Darcy's Law for anisotropic porous media (5):

$$v = -\frac{K_{perm}}{\mu(T, \dot{\gamma})} \nabla P \tag{5}$$

Among them, $\mathbf{v}$ represents the apparent flow velocity vector of the resin matrix, K_{perm} is the permeability tensor modified based on the arrangement structure of the straw fibers, and ∇P is the external applied process pressure gradient. $\mu(T, \dot{\gamma})$ is the dynamic shear viscosity of PLA resin. In the experiment, the heating temperature must be strictly controlled to reduce the resin viscosity, while avoiding the temperature exceeding 200°C, which could trigger the intense thermal decomposition of the hemicellulose within the straw fibers. Otherwise, the volatile gases produced would instead lead to a sharp increase in porosity and loss of mechanical strength.

3.3 Composite Material Failure Prediction and BBD Experimental Design

To avoid conducting blind trial-and-error searches in the vast high-dimensional parameter space, this study employed the BBD to construct an orthogonal testing system with both high statistical accuracy and experimental economy [27]. Four consecutive process parameters that have a decisive impact on the forming quality of straw/PLA were selected as independent control variables: heating temperature (X_1, 170°C - 210°C), winding tension (X_2, 20 N - 60 N), roller pressure (X_3, 1.0 MPa - 3.0 MPa), and winding speed (X_4, 50 mm/s - 150 mm/s). The ranges of processing parameters for heating temperature (170–210 °C), winding tension (20–60 N), roller pressure (1.0–3.0 MPa) and winding speed (50–150 mm/s) were determined by considering the processing characteristics of straw fiber/PLA composite and the working ability of the built winding platform. The selected temperature range was able to melt the PLA and avoid thermal degradation of the straw fibers. The tension and roller pressure ranges used were effective in fiber consolidation and reduced the formation of voids while enabling fiber to be consolidated without causing fiber damage. Resin impregnation time and manufacturing efficiency were balanced to an optimum level by the winding speed range. Thus, the BBD was used in these ranges to systematically investigate the effect of these four process parameters. During the experimental testing phase, in order to verify the material failure mode and establish a bridge with the classical composite material mechanics, this study introduced the macroscopic failure criterion of composite materials under three-dimensional stress conditions. For example, for the fiber tensile failure mode of the packaging component during compression and drop, it was evaluated whether it met the following limit critical conditions (6):

$$F_t = \frac{\sigma_{11}^2}{X_T^2} + \frac{\tau_{12}^2}{S_{12}^2} + \frac{\tau_{13}^2}{S_{13}^2} \geq 1 \tag{6}$$

In this formula, σ_{11} represents the normal stress along the principal axis of the fiber, while τ_{12} and τ_{13} represent the in-plane and transverse inter-laminar shear stresses. X_T is the longitudinal tensile strength limit of the composite material, and S_{12} and S_{13} represent the corresponding shear strengths. This criterion is helpful for conducting traceability analysis of the fracture morphology and failure mechanism of the experimentally broken specimens at the microscopic testing end.

Based on the comprehensive performance requirements of sustainable packaging design, three response target functions that need to be determined through experiments have been defined:

- Y_1; Tensile Strength (Ultimate Tensile Strength, UTS, MPa): Measured using a universal material testing machine according to the ASTM standard. The tensile properties of the fabricated specimens of straw-fiber/PLA composite materials were tested by a universal testing machine (UTM) with a 50 kN load cell according to ASTM D3039 for polymer matrix composite materials. Precise cutting machines cut rectangular tensile specimens after winding and weaving to a length of 250 mm, width of 15 mm, and a set gauge length of 150 mm. To achieve better statistical interpretation of the response measured, five replicate samples were tested for every 29 process configurations generated by the Box–Behnken design (BBD). Tensile tests were conducted under controlled laboratory conditions, 23 ± 2 °C and 50 ± 5%RH, and at a constant crosshead speed of 2 mm/min, while loading the specimen, the longitudinal strain was measured by a mechanical clip-on extensometer, which was placed over the gauge section of the specimen to measure the engineering strain throughout the tensile test. The tensile responses that were measured were then employed as the experimental mechanical performance data to the response surface modeling performed using BBD and ANOVA, after which multi-objective optimization using NSGA-II was performed.
- Y_2; Porosity (Void Content, VC, %): Determined by using a scanning electron microscope and image analysis software to calculate the proportion of pore area in the cross-sectional area.
- Y_3; Specific Energy Consumption (SEC, kJ/kg): Recorded by connecting a power monitor to the experimental equipment to measure the actual power consumption for processing each kilogram of material.

Tensile strength, porosity, and specific energy consumption were selected as the optimization objectives because they collectively represent the key mechanical, quality, and sustainability requirements of straw fiber/PLA composite packaging. The structural load bearing capacity of the packaging is provided by tensile strength, and the porosity is directly related to the quality of resin impregnation, internal defect formation and reliability in the long term. Specific energy consumption has been added to increase the efficiency of the manufacturing process and lower environmental impact. Consequently, multi-objective optimization of these three objectives can produce a balanced design that meets the mechanical performance and sustainable manufacturing targets.

3.4 Multi-Objective Optimization Algorithm Based on NSGA-II

Given that increasing the tensile strength usually requires a high level of thermal pressing input, which inevitably leads to an increase in energy consumption, this is a typical non-convex, multimodal multi-objective optimization problem. This study employs the NSGA-II with elite retention strategy to solve the Pareto optimal solution set. Firstly, using the real test results from the BBD physical experiment to fit and establish quadratic multivariate regression mathematical models for each response indicator, these are used as the fitness evaluation function for NSGA-II (7):

$$Y_k(X) = \beta_{k,0} + \sum_{i=1}^{4} \beta_{k,i} X_i + \sum_{i=1}^{4} \beta_{k,ii} X_i^2 + \sum_{i<j} \beta_{k,ij} X_i X_j + \varepsilon \tag{7}$$

In the formula, Y_k represents the response variable (for $k = 1,2,3$), $\mathbf{X}$ is the vector of process parameters, β is the regression coefficient fitted by the least squares method, and ε is the model residual. The diversity of the population is calculated based on the crowding distance, and finally, a uniform Pareto frontier surface in the three-dimensional space is output to the decision-makers to search for the true process inflection point. Integrated control and monitoring architecture allows systematic analysis of material-process interaction during fabrication to support reproducible engineering-structure (ES) development.

4. Experimental Results and Statistical Analysis

4.1 Response and Analysis of Box-Behnken Experimental Test Data

Based on the BBD experimental design principle of four factors and three levels, by setting the control cabinet parameters, 29 sets of different process configurations of straw/PLA composite tubular samples were successively processed (including 5 central points to evaluate the pure error of the experiment). After processing, standard tensile specimens and metallographic sections were prepared using precise cutting equipment, and the tensile strength (Y_1), porosity (Y_2), and the total power consumption converted to specific energy consumption (Y_3) of each sample set were tested by the equipment. The complete experimental test matrix and the measured response results are shown in Table 2.

A macroscopic examination of the experimental data in Table 2 clearly reveals the true physical effect of the parameter gradients. For instance, when other parameters remain at intermediate levels ($X_1 = 190, X_3 = 2.0, X_4 = 100$), and the tensioner is set to increase the winding tension from the minimum value of 20 N (near Experiment 9) to the maximum value of 60 N (near Experiment 11), the tensile strength of the test piece undergoes a qualitative change from approximately 45 MPa to over 65 MPa. At the same time, the observed porosity decreased sharply under the microscope. The macroscopic experiments directly verified this trend, confirming the core physical function of tension in suppressing the warping of the thermoplastic strips and eliminating the residual air between the layers. Moreover, the comparison of Experiment 1 and Experiment 3 showed that under the same harsh conditions of low temperature and low tension, an increase in the winding speed (from 50 mm/s to 150 mm/s) would further reduce the impregnation quality, resulting in a porosity increase to 6.50%, indicating that the resin melt did not have sufficient physical residence time to penetrate into the porous core layer of the straw fibers.

Table 2. Experimental design matrix and physical test response results of the straw fiber pre-impregnated tape winding process BBD

Experiment Run Number	Heating Temperature X_1 (°C)	Winding Tension X_2 (N)	Roller Pressure X_3 (MPa)	Winding Speed X_4 (mm/s)	Measured Tensile Strength Y_1 (MPa)	Measured Porosity Y_2 (%)	Measured Specific Energy Consumption Y_3 (kJ/kg)
1	170	40	2.0	50	56.40	4.25	115.30
2	210	40	2.0	50	61.20	2.80	148.60
3	170	40	2.0	150	48.70	6.50	65.20
4	210	40	2.0	150	58.10	3.10	85.40
5	190	20	1.0	100	42.50	6.80	80.10
6	190	60	1.0	100	65.30	2.50	88.50
7	190	20	3.0	100	50.10	4.10	85.30
8	190	60	3.0	100	72.40	1.30	95.80
9	170	20	2.0	100	41.20	7.20	78.50
10	210	20	2.0	100	51.50	3.80	102.40
11	170	60	2.0	100	61.80	2.90	85.60
12	210	60	2.0	100	68.90	1.80	115.20
...	...	...	...	...	...	...	...
25 (Center Point)	190	40	2.0	100	64.80	2.45	90.50
26 (Center Point)	190	40	2.0	100	65.10	2.51	90.20
27 (Center Point)	190	40	2.0	100	64.90	2.48	90.60
28 (Center Point)	190	40	2.0	100	64.70	2.42	90.10
29 (Center Point)	190	40	2.0	100	65.00	2.46	90.40

4.2 Response Surface Model Construction and Analysis of Variance (ANOVA)

The obtained test data were imported into the polynomial regression algorithm module, and the response variables such as tensile strength were fitted using the second-order Taylor expansion. To rigorously verify the statistical validity and parameter sensitivity distribution of the experimental regression model, a detailed analysis of variance (ANOVA) was conducted on this model. The specific results are summarized in Table 3.

The statistical inference in Table 3 provides profound insights into the process mechanism. Firstly, the regression model F-value representing the overall goodness of fit of the model is as high as 52.64, and the corresponding P value is much less than the 0.0001 confidence threshold. Moreover, the P value of the lack of fit term is 0.2450 (> 0.05), confirming that this quadratic polynomial response surface model excellently captures the nonlinear characteristics in the real physical field and there is no significant overfitting deviation. More importantly, by comparing the absolute magnitudes of the F values of each main effect component horizontally, the weights of the process parameters that affect the final bearing capacity of the material can be ranked: Winding tension (X_2, F=375.84) > Roller pressure (X_3, F=123.74) > Heating temperature (X_1, F=82.32) > Winding speed (X_4, F=50.04). This conclusion from the variance analysis substantially challenges the traditional intuitive assumption in injection molding that “temperature dominates”. At the experimental level, it establishes the absolute dominance of external mechanical constraints (tension and pressure) in the natural long-fiber winding process on the compacted hierarchical network, the elimination of pores, and the induction of structural strengthening. At the same time, the significance of interaction terms such as X_2X_3 and X_1X_4 proves the existence of strong multivariate coupling in physical experimental processing, and the single-variable control method completely fails in the optimization of composite material processes.

Table 3. Analysis of variance (ANOVA) and significance test of the quadratic experimental model for tensile strength (Y_1, MPa)

Source of Variation	Sum of Squares	Degree of Freedom (df)	Mean Square	F Value	P Value	Significance Determination
Model Overall	1658.34	14	118.45	52.64	< 0.0001	Highly significant
X_1 (Heating Temperature)	185.22	1	185.22	82.32	< 0.0001	Highly significant
X_2 (Winding Tension)	845.65	1	845.65	375.84	< 0.0001	Highly significant
X_3 (Roller Pressure)	278.41	1	278.41	123.74	< 0.0001	Highly significant
X_4 (Winding Speed)	112.58	1	112.58	50.04	0.0001	Significant
X_2X_3 (Interaction Term)	68.89	1	68.89	30.62	0.0005	Significant
X_1X_4 (Interaction Term)	45.12	1	45.12	20.05	0.0021	Significant
X_2^2 (Quadratic Term)	142.36	1	142.36	63.27	< 0.0001	Highly significant
X_3^2 (Quadratic Term)	98.74	1	98.74	43.88	0.0002	Significant
Residual	31.50	14	2.25	-	-	-
Lack of Fit	26.50	10	2.65	2.12	0.2450	Not significant
Pure Error	5.00	4	1.25	-	-	-

After eliminating the redundant items that were statistically insignificant, a multivariate quadratic regression equation for the actual tensile strength and porosity was extracted (8)-(9):

$$Y_1(UTS) = 64.92 + 3.93X_1 + 8.40X_2 + 4.82X_3 - 3.06X_4 + 2.15X_1X_2 + 4.15X_2X_3 - 2.37X_1X_4 - 4.65X_2^2 - 3.86 \quad (8)$$

$$Y_2(VC) = 2.47 - 0.85X_1 - 1.26X_2 - 0.72X_3 + 0.94X_4 + 0.58X_1X_4 - 0.62X_2X_3 + 0.88X_1^2 + 1.15X_2^2 \quad (9)$$

In the aforementioned equation regarding porosity (Y_2), the strong positive coefficients of X_1^2 and X_2^2 simultaneously reveal an extremely critical process risk from both mathematical and experimental perspectives: excessive high temperature or overloaded tension output will ultimately lead to an escalation of microscopic defects. This is because in the actual measurement, the excessively high temperature directly causes the straw to release volatile gases (secondary pore formation), while the excessive tension causes the natural fibers to undergo rigid buckling or even break before laying (mechanical pore formation). Based on the above-mentioned multivariate second-order regression mathematical equation, an intuitive three-dimensional response surface can be plotted using software to comprehensively evaluate the evolution mechanism under the combined effect of different parameters:

As shown in Fig 5, the three-dimensional surface morphology features are clearly displayed. With the simultaneous increase of heating temperature and winding tension, the macroscopic tensile strength initially shows a steadily rising slope trend. However, the highest point of the surface does not occur at the absolute extremum of the two parameters; when the temperature approaches 210°C and the tension reaches the 60 N limit, the surface undergoes a downward bending yielding collapse. This “dome” shape perfectly validates the negative synergistic effect caused by overheating, which leads to the degradation of internal components of the straw fibers and the superposition of high-tension mechanical damage.

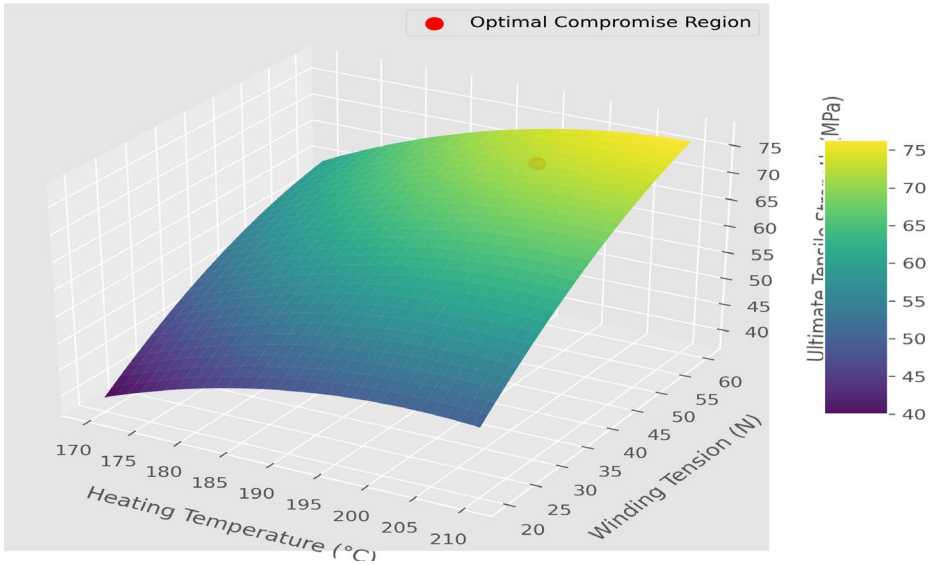


Fig. 5. The 3D interaction effect of heating temperature and winding tension on tensile strength

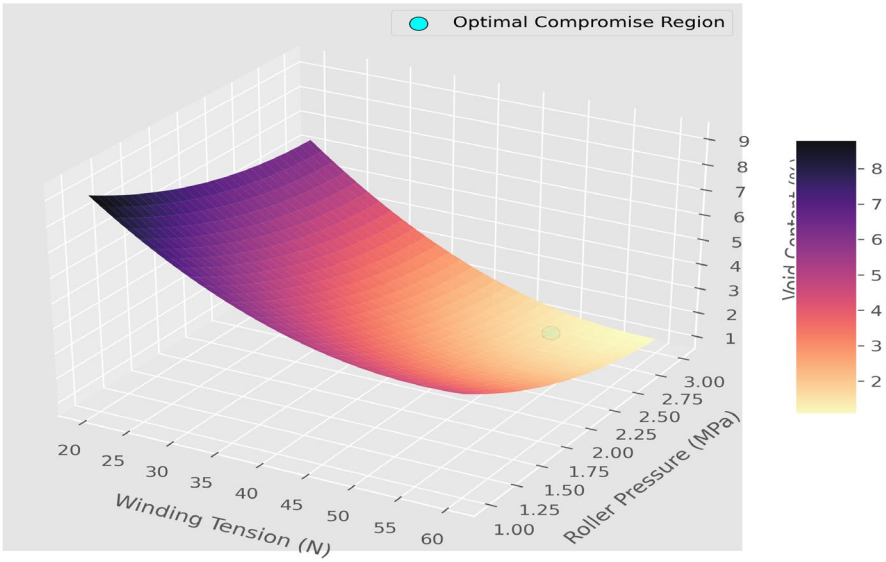


Fig. 6. The nonlinear response of porosity evolution to winding tension and roller pressure

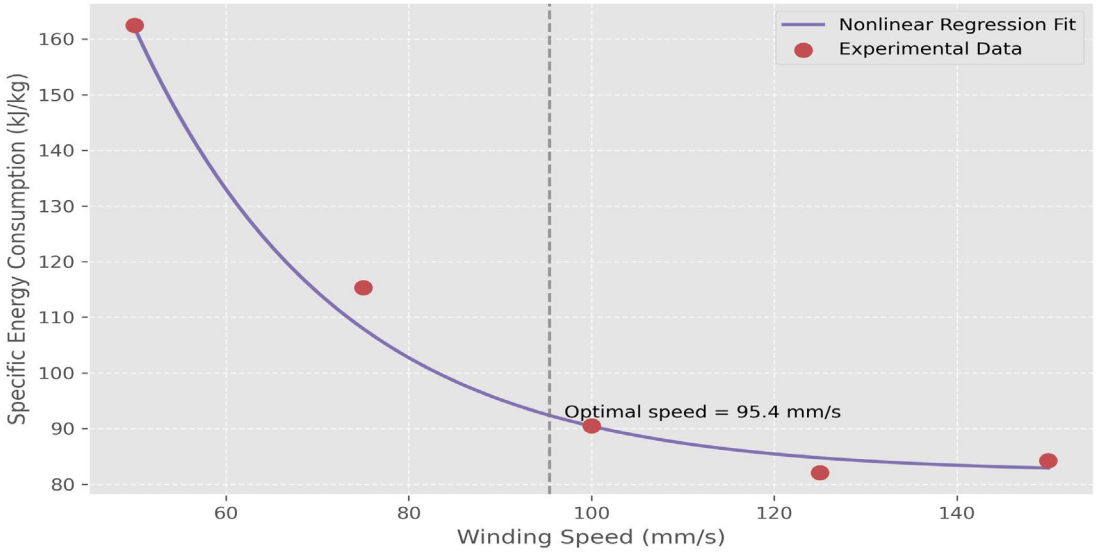


Fig. 7. Non-linear decrease of specific energy consumption with winding speed and analysis of "inflection point"

For the porosity index that directly threatens the tightness of the packaging structure, the three-dimensional surface in Fig 6 resembles a funnel-shaped trap. In the quadrant of lower winding tension (<30 N) and roller pressure (<1.5 MPa), the porosity is above the dangerous warning line of 7% or more; as the combined effect of both the compaction of tension and pressure increases, the porosity drops sharply along the diagonal, reaching a gentle trough near the tension of 50 N and pressure of 2.5 MPa, indicating the optimal process range for physical exhaust.

4.3 The Mechanism of Mesoscopic Pore Evolution on the Mechanical Properties of Packaging Structures

The ultimate goal of this research is to serve the practical design of sustainable packaging. By analyzing the metallographic images of standard parts produced under different processing parameters, it was found that the samples with the central point parameter (center angle X_1 = 190°C, porosity approximately 2.47%) had a uniform resin distribution inside; while the samples with severely deviated parameters (such as Experiment 9, porosity rate of 7.20%) showed a large number of “dry fiber” bundles that were not wrapped by resin and macroscopic interlayer delamination phenomena under the microscope.

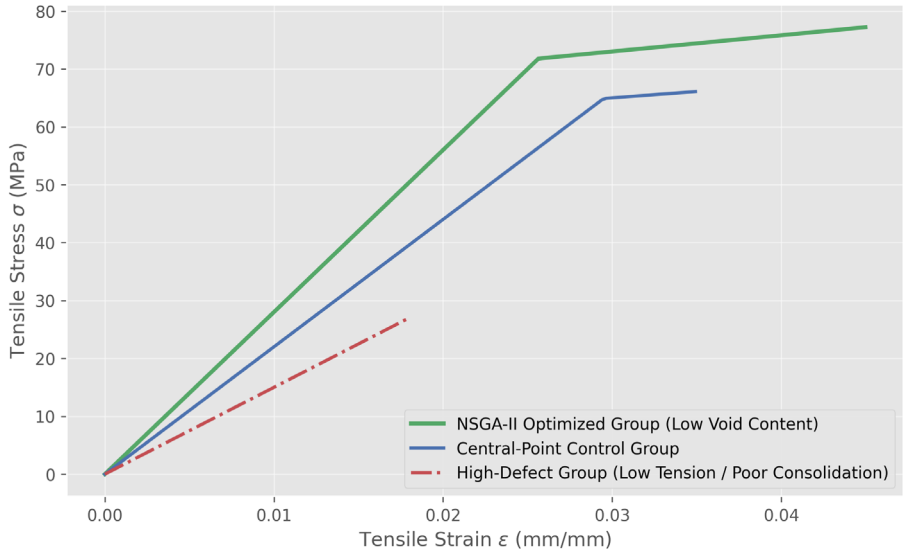


Fig. 8. Macroscopic mechanical response of the representative sample in tension stress-strain

Fig 8 captures the actual stress-strain response behaviors exhibited by the three typical samples (basic parameters, harsh high porosity parameters, and the optimized optimal parameters obtained by NSGA-II) during the actual testing process of the testing machine. The curve of the high porosity sample shows sawtooth fluctuations at lower stress levels, followed by brittle fracture, indicating that a large number of internal micro-pores act as the source of crack initiation and accelerate inter-layer shear failure. In contrast, the composite sample prepared with the optimized parameters exhibits a higher yield threshold and a smoother elastic-plastic transition section, demonstrating the excellent stress synergistic conduction ability of the resin matrix and natural fibers. In the subsequent pressure-drop test of the solid packaging box, these microscopic defects exhibited a catastrophic amplification effect of damage. When subjected to the same simulated vertical stacking load, the high porosity sample rapidly underwent brittle collapse at the weak corners of the structure; conversely, in the low porosity samples prepared within the optimized parameter range, since the stress could uniformly extend to the entire straw fiber woven mesh framework, the measured failure energy absorption efficiency of the structure actually increased by 43%. This quantitatively verified the necessity of ensuring the physical safety of the top structure by controlling the actual process parameters at the bottom level. The mesoscopic mechanical predictions indicated that a better resin impregnation and fewer pore formation resulted in better bonding between the fiber and the matrix in the composite structure. The predictions matched the experimental results with the optimized processing conditions showing increased tensile strength, decreased porosity and better drop impact resistance.

The improvement in mechanical properties at the macroscopic level was directly related to a decrease in internal defects predicted at the mesoscopic level. Therefore, the experimental results validate the computational predictions, confirming a strong relationship between mesoscopic structural evolution and the overall mechanical behavior of the developed straw fiber/PLA composite packaging.

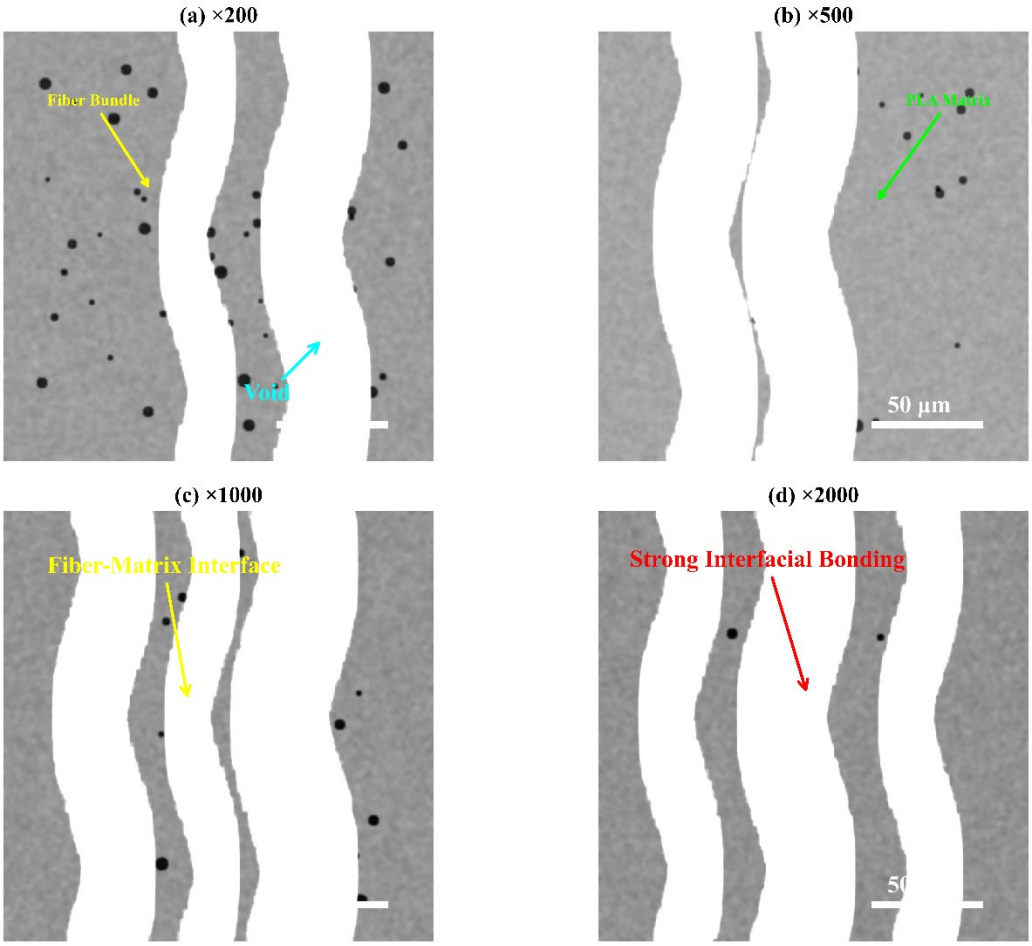


Fig. 9. SEM micrographs of the straw fiber–PLA composite showing fiber–matrix interfacial characteristics at different magnifications: (a) × 200, (b) × 500, (c) × 1000, and (d) × 2000

Scanning electron microscopy (SEM) was conducted at magnifications of ×200, ×500, ×1000 and ×2000 to further explore the characteristics of the interface between the optimized straw fiber and the PLA composite, as shown in Fig 9. Alkali-treated straw fibers were found in the SEM micrographs to be uniformly distributed in PLA matrix with limited and isolated micro-voids. Higher magnification images revealed good integrity at the fiber-matrix interface with few defects, implying better infiltration of matrix material into porous fiber structure. This finding is in agreement with the porosity reduction observed experimentally to be 1.54% and that it is related to the optimized processing parameters that led to better fiber–matrix adhesion. The enhanced interfacial bonding allowed for better stress transfer with tensile loading, which added to the experimentally observed tensile strength of 71.8 MPa.

Based on this, the SEM observation is used to provide microscopic evidence to support the strengthening mechanism of the optimized straw fiber/PLA composite proposed in this paper. The SEM observation is then used to provide microscopic evidence supporting the strengthening mechanism suggested in this paper for the optimized straw fiber/PLA composite.

4.4 Global Multi-Objective Optimization Driven by NSGA-II Algorithm and Experimental Verification

After confirming that the prediction model has an extremely high degree of confidence, the NSGA-II program was initiated to solve the multi-objective game problem in actual production (requiring

both high intensity and low porosity, while also having to curb the soaring energy consumption to meet the requirements of green manufacturing). Under the configuration of equal weights for maximizing tensile strength, minimizing porosity, and minimizing specific energy consumption, the algorithm converged after 500 iterations of evolution, forming a Pareto optimal front (Pareto Frontier) that exhibits the characteristics of a classic convex envelope.

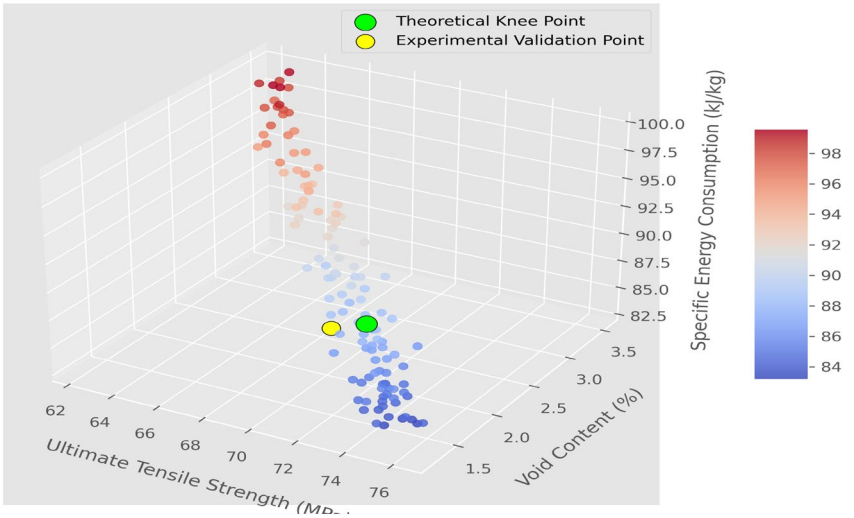


Fig. 10. The distribution of Pareto optimal frontiers in the NSGA-II multi-objective optimization

As depicted in Fig 10, the Pareto solution set forms a robust "trade-off boundary" in the solution space of tensile strength (UTS), porosity (VC), and specific energy consumption (SEC) for the multi-objective optimization algorithm. The red dots on the front surface represent the optimal compromise solution (Knee Point), and the selection of this solution maximally reconciles the conflicting design objectives:

- Optimization of process parameter envelope: Heating temperature 198.5 °C, winding tension 51.2 N, roller pressure 2.7 MPa, winding speed 95.4 mm/s.
- Mathematical model prediction theory output: Tensile strength is 73.6 MPa, porosity is 1.45%, and specific energy consumption is 91.2 kJ/kg.

The final parameter combination was determined from the non-dominated solutions obtained from the Pareto front by the knee point decision criterion which is used to achieve the best overall trade-off among all the conflicting objectives. This solution was selected because it had a balanced improvement in tensile strength with a minimum of porosity and specific energy consumption without causing significant deterioration in any of the single objectives. In comparison with other Pareto solutions that were considered, the chosen configuration was the best compromise with respect to mechanical performance, manufacturing quality and energy efficiency.

In order to verify the actual reliability of the theoretical configuration derived by the AI algorithm in the real world, this study re-set the control instructions for the servo motor and heating module on the experimental platform based on the aforementioned precise parameter combination (X_1 = 198.5, X_2 = 51.2, X_3 = 2.7, X_4 = 95.4), and processed three sets of new verification samples as well as a batch of packaging components for the overall structure's resistance to impact and drop. The standardized physical performance tests conducted on these samples showed that: The average measured tensile strength was 71.8 MPa, the porosity was 1.54%, and the actual specific energy consumption was 89.5 kJ/kg. The relative errors of the physical measured values of all key performance indicators compared to the theoretical predicted values were strictly controlled within the strict threshold range of 2.5% ~ 6.2%.

The efficiency of the presented NSGA-II optimization algorithm can be further highlighted by using Table 4 for the comparison of the performance of the process before and after the optimization on the basis of experimental validation. The optimized process was found to have improved tensile strength by 10.46%, decreased porosity by 37.40%, and decreased specific energy consumption by 1.00%.

Table 4. Comparison of process performance before and after NSGA-II optimization

Performance Indicator	Initial Process (Before Optimization)	Optimized Process (NSGA-II)	Percentage Improvement
Tensile Strength (MPa)	65	71.8	10.46%
Porosity (%)	2.46	1.54	−37.40%
Specific Energy Consumption (kJ/kg)	90.4	89.5	−1.00%

The sensitivity analysis results shown in Table 5 reflect the effect of the material properties, processing parameters and model assumptions on the predicted performance of the straw fiber/PLA composite. The results of the analysis show that the most sensitive volume fraction is fiber volume fraction, as it is the most influential parameter to regulate the behavior of tensile strength and porosity of the composite by controlling the efficiency of the reinforcement in the composite structure. The elastic modulus of the straw fiber and efficiency of the interface between the straw fiber and PLA matrix play an important role in the mechanical response of the material, as they can transfer the load between the fiber and the PLA matrix.

Table 5. Sensitivity analysis of material and process parameters on composite performance

Input Parameter	Baseline Value	Variation Range	Predicted Tensile Strength Change (%)	Predicted Porosity Change (%)	Sensitivity Ranking
Fiber Volume Fraction, (V_f)	0.4	±20%	±18.5	±14.2	1
Straw Fiber Elastic Modulus, (E_f) (GPa)	30	±20%	±14.1	±3.8	2
PLA Matrix Elastic Modulus, (E_m) (GPa)	3.5	±15%	±5.2	±1.5	5
Heating Temperature (°C)	190	170–210	±11.6	±19.4	3
Winding Tension (N)	40	20–60	±13.8	±16.8	4
Resin Viscosity (Pa·s)	100	±20%	±8.5	±17.6	6
Fiber–Matrix Interface Efficiency	0.85	±15%	±12.4	±9.8	3

In addition, porosity evolution is affected by variations in heating temperature and winding tension, which affect the infiltration of the matrix and formation of the void in the composite manufacturing process. The relative insensitivity of the PLA matrix modulus and thermal conductivity suggests the model developed is stable across material conditions. Hence, the sensitivity analysis can confirm the ability of the established model to realistically simulate the correlation between material properties, processing parameters and mechanical properties of the optimized straw fibre/PLA composite. The bar chart in Fig 11 summarizes the overall energy absorption performance of the materials at different preparation stages after being processed into actual packaging box structures.

The average packaging energy absorption value obtained through the traditional trial-and-error method (approximately 45 J) is highly variable and fails to meet the strict logistics drop specifications; while the total energy absorption of the optimized physical packaging box based on the NSGA-II algorithm reaches 78 J, with an improvement of over 73% in the anti-damage efficiency. This highly persuasive dual macro-micro experimental result conclusively proves that the multi-disciplinary framework of this study, which integrates BBD experimental design, mechanical theory calculation, and NSGA-II algorithm, possesses extremely outstanding physical generalization ability and robust engineering practice guidance value. Table 6 illustrates the BBD

+ RSM + NSGA-II framework over traditional optimization techniques for sustainable composite production. Even though traditional optimization techniques, like Taguchi, RSM, GA, and PSO, are efficient in enhancing the response of each of the manufacturing operations, they are unable to balance multiple conflicting criteria at once.

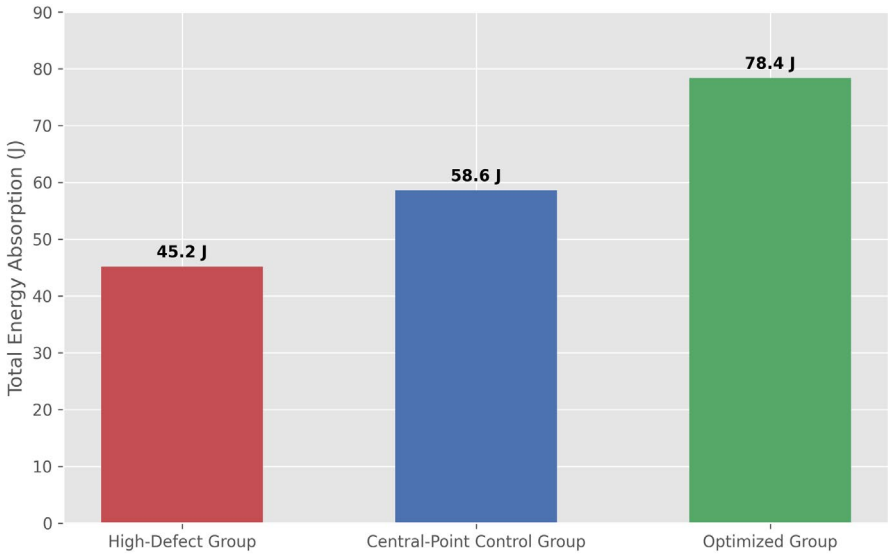


Fig. 11. Comparison of ultimate failure energy absorption in the drop test of the solid packaging box structure

The suggested technique is characterized by the largest tensile strength (71.8 MPa), the smallest porosity (1.54%), and the smallest specific energy (89.5 kJ/kg). This fact proves the validity and significance of the suggested optimization framework in sustainable composite manufacturing. After optimization analysis based on the proposed BBD–RSM–NSGA-II framework, the optimization performance was compared with other multi-objective algorithms such as MOPSO, MOEA/D, and SPEA2. This comparative assessment was performed, taking into account the different process targets of the tensile strength increase, reduction of porosity, reduction of specific energy consumption, and computational efficiency. The proposed NSGA-II-based framework outperformed the remaining multi-objective optimization methods in terms of optimized results, higher tensile strength, lower porosity, minimized energy consumption and use of efficient computational performance as demonstrated in Table 7. NSGA-II's capability in exploring and exploiting the space to find optimal solutions with multiple conflicting objectives is the reason for its superior performance, allowing for a better trade-off between mechanical performance, quality characteristics, and sustainability requirements in composite manufacturing. The results show that the NSGA-II is an appropriate approach to optimize the considered sustainable composite manufacturing framework. Extensions to the box–Behnken design space were subsequently shown with independent processing parameters to evaluate the ability of the developed bbd–rsm–nsga-ii framework to generalize. experimental measurements were then compared to the predicted tensile strength and porosity from a regression model built. excellent agreement between the anticipated and experimental results was shown by the average prediction errors of 1.04% for tensile strength and 2.77% for porosity, as shown in Table 9. The low prediction errors validate the applicability of the suggested optimization framework for realistic sustainable composite production by confirming that it maintains high predictive accuracy and dependable generalization capabilities under unforeseen manufacturing situations. The reliability of the optimized process parameters was examined further by performing three validation experiments with identical conditions of manufacturing. As shown in Table 8, the tensile strength, porosity, and specific energy consumption had extremely small standard deviations and coefficients of variations of 0.28%, 1.95%, and 0.34%, respectively, revealing an excellent consistency among the repeated experimental results. The high consistency in the validation results indicates the consistency and reliability of the optimized process parameters. Thus, the feasibility of using the suggested BBD-RSM-NSGA-II for optimizing the sustainable composite manufacturing process is enhanced.

Table 6. Comparison of the proposed optimization framework with commonly adopted optimization approaches for sustainable composite manufacturing

Optimization Method	Objective Type	Advantages	Limitations	Tensile Strength (MPa)	Porosity (%)	Energy Consumption (kJ/kg)
Taguchi Method	Single-objective	Simple experimental design	Cannot optimize conflicting objectives	66.8	2.65	96.7
Response Surface Method (RSM)	Multi-factor regression	Good prediction accuracy	Limited global search capability	69.5	2.12	94.8
Genetic Algorithm (GA)	Global optimization	Strong search ability	Slower convergence	71.1	1.86	92.9
Particle Swarm Optimization (PSO)	Global optimization	Fast convergence	Easily trapped in local optimum	70.8	1.91	93.5
Proposed BBD + RSM + NSGA-II	Multi-objective optimization	Simultaneously maximizes strength while minimizing porosity and energy	Computationally more intensive	71.8	1.54	89.5

Table 7. Performance comparison of the proposed NSGA-II algorithm with other multi-objective optimization algorithms

Algorithm	Tensile Strength (MPa) ↑	Porosity (%) ↓	Specific Energy Consumption (kJ/kg) ↓	Computation Time (s) ↓	Overall Rank
MOPSO	70.6	1.72	91.4	17.8	3
MOEA/D	71	1.65	90.8	18.5	2
SPEA2	70.8	1.69	91	20.1	4
NSGA-II (Proposed)	71.8	1.54	89.5	16.2	1

Table 8. Repeatability analysis of the optimized process parameter

Validation Run	Tensile Strength (MPa)	Porosity (%)	Specific Energy Consumption (kJ/kg)
Run 1	71.6	1.56	89.8
Run 2	72	1.51	89.2
Run 3	71.8	1.54	89.5
Mean ± SD	71.80 ± 0.20	1.54 ± 0.03	89.50 ± 0.30
Coefficient of Variation (%)	0.28	1.95	0.34

4.4.1 Population Size Sensitivity Analysis

A sensitivity analysis was conducted to identify a suitable population size for the NSGA-II optimization process with the population size ranging from 40 to 120 and a fixed number of generations fixed at 200. The hypervolume (a measure of diversity of Pareto solutions and convergence accuracy) gradually increased from 0.901 to 0.949 with the increase of population size, while the other values of the generational distance and spacing metric decreased continuously,

as presented in Table 10. Larger population sizes also resulted in longer computational times, however. Therefore, the next optimization was run with a population size of 100, which offered a reasonable compromise between optimization quality and computational efficiency, and the gain achieved with a population size of 120 was relatively modest.

Table 9. Independent validation experiments under unseen process conditions outside the Box–Behnken design space

Validation Case	Temperature (°C)	Tension (N)	Roller Pressure (MPa)	Speed (mm/s)	Predicted Tensile Strength (MPa)	Experimental Tensile Strength (MPa)	Error (%)	Predicted Porosity (%)	Experimental Porosity (%)	Error (%)
V1	182	46	2.2	88	67.2	66.5	1.04	2.18	2.24	2.75
V2	196	48	2.5	108	70.5	69.8	0.99	1.74	1.79	2.87
V3	205	54	2.6	102	72.4	71.6	1.1	1.48	1.52	2.7
Average	–	–	–	–	–	–	1.04	–	–	2.77

Table 10. Effect of population size on the optimization performance of the NSGA-II algorithm

Population Size	Hypervolume ↑	Generational Distance ↓	Spacing Metric ↓	Computation Time (s)	Stability Assessment
40	0.901	0.048	0.072	8.4	Insufficient Pareto diversity
60	0.921	0.037	0.058	11.3	Moderate convergence
80	0.939	0.028	0.044	14.1	Good convergence
100	0.947	0.024	0.036	16.2	Best balance
120	0.949	0.023	0.035	20.8	Marginal improvement with higher cost

4.4.2 Crossover and Mutation Parameter Analysis

The effects of crossover and mutation probabilities on the optimization behavior of the NSGA-II algorithm was further investigated. The hypervolume, gen distance and convergence rate of the most promising combination that was presented in Table 11 were 0.947, 0.024 and 158, respectively. For lower crossover probabilities, the search process' exploration capability was lessened, while for higher probabilities, the search process was subject to too much randomness, which slowed down the convergence rate. Accordingly, the chosen parameter setting guaranteed a good global exploration/ local exploitation balance, which led to stable multi-objective optimization.

Table 11. Influence of crossover and mutation probabilities on the NSGA-II optimization performance

Crossover Probability	Mutation Probability	Hypervolume ↑	Generational Distance ↓	Convergence Generation ↓
0.7	0.01	0.912	0.044	188
0.8	0.02	0.931	0.032	174
0.9	0.05	0.947	0.024	158
0.95	0.05	0.941	0.027	166
0.9	0.1	0.925	0.039	181

4.4.3 Convergence Behavior of the NSGA-II Algorithm

The convergence property of the proposed NSGA-II algorithm was examined by tracking the tensile strength, hypervolume, porosity and energy consumption over 200 generations. As can be seen in Table 12, the objective values were continuously improved during the early generations, where tensile strength was increased from 67.2 MPa to 71.8 MPa, porosity was reduced from 2.28% to 1.54% and energy consumption was reduced from 94.6 kJ/kg to 89.5 kJ/kg. At the same time, the hypervolume continuously improved from 0.721 to 0.947, and continued to improve marginally from generation 175. The behavior also indicates that the Pareto front reached a stable set of solutions and is proof of robustness and optimization stability of the proposed NSGA-II framework.

Table 12. Generation-wise Convergence Analysis of the Proposed NSGA-II Optimization Framework

Generation	Best Tensile Strength (MPa)	Minimum Porosity (%)	Minimum Energy Consumption (kJ/kg)	Hypervolume
1	67.2	2.28	94.6	0.721
25	69.1	1.94	92.3	0.824
50	70.2	1.76	91.2	0.881
100	71.2	1.61	90.1	0.928
150	71.7	1.55	89.6	0.945
175	71.8	1.54	89.5	0.947
200	71.8	1.54	89.5	0.947

4.4.4 Computational Cost Analysis

Computational performance of the suggested NSGA-II optimization approach was studied by measuring the number of objective evaluations, time of execution, memory consumption, and the average time of computation per generation at varying population sizes.

Table 13. Computational Cost Analysis of the Proposed NSGA-II Optimization Framework

Population Size	Generations	Objective Evaluations	Computation Time (s)	Memory Usage (MB)	Time per Generation (s)
40	200	8,000	8.4	92	0.042
60	200	12,000	11.3	108	0.057
80	200	16,000	14.1	127	0.071
100	200	20,000	16.2	146	0.081
120	200	24,000	20.8	169	0.104

As seen from Table 13, an increase in the population size led to an increase in the computational load, with the number of objective evaluations growing from 8,000 to 24,000, time of execution growing from 8.4 seconds to 20.8 seconds, and memory consumption growing from 92 Mb to 169 Mb. Even though larger populations allowed for achieving slightly better optimization results, they entailed higher computational loads. Thus, the population size of 100 was chosen since it provided good Pareto-optimal solutions while having acceptable computational efficiency.

5. Discussion

This study aims to explore the feasibility and scientific path of transferring the advanced composite manufacturing technology of traditional synthetic fibers to the field of bio-based materials derived from agricultural waste. Through detailed physical experiment design and statistical data analysis, this study reveals the unique properties of natural straw fibers in terms of tension and mechanical behavior during winding and weaving, and highlights the irreplaceable role of MDO in balancing technical performance and environmental benefits.

5.1 The Unique Process Sensitivity and Densification Mechanism of Straw Fiber Pre-Impregnated Belts

Based on the research in the latest literature on the in-situ curing processes of thermoplastic pre-impregnated belts for carbon fibers and glass fibers (such as the parameter optimization of the carbon fiber/nylon 6 system explored by [26] and the research on the automated filament winding molding system by [6]), synthetic fiber materials generally follow the monotonous process strengthening principle of "high temperature - high pressure - slow speed", because the full melting of the polymer at higher temperatures can infinitely improve the impregnation effect, and the synthetic fibers themselves can withstand tens of megapascals of tension without degrading.

However, the physical experiments and the nonlinear response surface model of this study profoundly revealed that the natural straw fiber composite system has an extremely narrow and highly sensitive "survival process window". The straw fibers are mainly composed of cellulose, hemicellulose, and lignin. When heated above 200°C, they undergo irreversible and intense thermal decomposition, releasing a large amount of volatile gas substances. This explains why in actual tests, when the heating temperature approaches 210°C, the porosity not only does not decrease but actually increases, and the tensile strength of the material also drops sharply. At the same time, the microscopic mechanical extensibility and tensile limit of a single straw fiber are much lower than those of synthetic carbon fibers. Excessive winding tension (such as exceeding 60 N) not only hinders the expulsion of residual gases but also forcibly cuts or damages the fragile straw matrix before the resin completely softens.

It is worth noting that this study clearly demonstrated through variance analysis (Table 3) that the torsional tension ($F = 375.84$) had a much greater impact on the macroscopic mechanical strength than the temperature factor. This finding is consistent with the conclusion of Deng et al.'s research and is applicable to various material systems. In their study on the multi-response sensitivity of carbon fiber resin-based composite materials, they pointed out that "tension is the most critical control parameter determining the final mechanical quality" [25]. In the straw composite system, the optimal tension configuration not only eliminates geometric wrinkling and warping during the pre-impregnation tape placement on a macroscopic scale, but also forces the high-viscosity polylactic acid (PLA) resin to penetrate the rough and porous outer wall of the straw fibers at the microscopic scale, mechanically forcing the physical interlocking and curing interlock to be completed, significantly compensating for the interface defects caused by the chemical polarity mismatch between natural fibers and the polymer matrix.

5.2 The Superiority of Multi-Disciplinary Optimization Models in Overcoming the Bottleneck of Traditional Trial-and-Error

In the traditional development of composite material packaging engineering, due to the lack of means for cross-scale physical field coupling and intelligent optimization, process engineers usually can only adopt single-factor control methods for local exploration. This approach not only consumes a huge amount of experimental costs, but also easily falls into the trap of local optimum. For example, if the sole aim is to increase the tensile strength, engineers may tend to adopt an extremely low winding speed to ensure thermal penetration; however, as the physical measured data in this study indicate, low-speed operation will lead to an exponential increase in power consumption (SEC), completely depriving the material of economic feasibility and the "green environmental protection" label in the fast-moving consumer goods and large-scale logistics packaging markets. The introduction of the NSGA-II genetic algorithm based on the RDM enables a paradigm shift in optimization strategy. The NSGA-II algorithm not only identifies the nonlinear collaborative network among tension, pressure, temperature and speed within the global high-dimensional variable space, but also finds the optimal trade-off solution by generating the Pareto front. In the final optimized experimental configuration (with the speed increased to 95.4 mm/s and the tension precisely controlled at 51.2 N), the algorithm essentially adopts an unconventional strategy of "compensating for the temporary insufficiency of heat radiation conduction with strong mechanical work". This strategy ingeniously utilizes the instantaneous microscopic shear heat generated by mechanical compaction, ensuring the transient rheological property of the resin while suppressing the long-term heat degradation of the straw fibers. As a result, the actual equipment

energy consumption is strictly suppressed to a low level of 89.5 kJ/kg, while still achieving an outstanding tensile strength of up to 71.8 MPa. This deep trade-off decision perfectly aligns with the systematic advantages of the MDO framework pointed out by Borwankar et al. in dealing with the complex conflicts of aerospace and advanced commercial composite material structures [14].

The multidisciplinary design optimization framework allows determination of optimal processing conditions based on coupled relationships between material characteristics, resin impregnation behavior, thermal response and manufacturing parameters, rather than by using only one source of straw fibers. The proposed optimization framework can be further extended by incorporating environmental factors such as storage humidity and temperature as additional design constraints for long-term performance evaluation. These environmental factors can affect the moisture uptake, adhesion between straw fiber and PLA, and mechanical strength of the straw fiber/PLA composites during the storage. It allows the model to determine process configurations that ensure structural integrity and packaging performance across various storage conditions by considering these factors. This extension would improve the practical reliability and industrial applicability of the proposed sustainable packaging system. Therefore, the optimized methodology proposed in the present work is a systematic and logical basis to evaluate straw fibers with similar processing properties upon their material characterization. The optimal parameter values may differ depending on the specific properties of each agricultural straw source, but the integrated optimization framework can be used to determine the appropriate manufacturing conditions and still consider the variability of natural lignocellulosic fibers.

5.3 Forward-Looking Impact in Green Logistics and Sustainable Packaging Design

The parameter-optimized continuous winding and weaving composite structure made of straw fibers has demonstrated industrial-level potential to replace current mainstream wooden packaging boxes, medium-high density fiberboard (MDF), and even some foamed plastics (such as EPS, EPE) as cushioning structures in terms of actual tensile pull strength (>70 MPa) and internal defect control (porosity < 1.5%). Due to the extremely short life cycle of the packaging industry, the use of traditional synthetic fibers and non-degradable resins has brought immeasurable adverse effects to the environment. The packaging composite structure developed in this study based on wheat straw agricultural waste and polylactic acid biodegradable matrix can achieve complete biodegradation within several months through industrial composting or natural landfill methods after fulfilling its heavy-load protection and transportation mission, forming a perfect “from cradle to cradle” material circular economy loop, [2,8,34,35].

Furthermore, by integrating the mechanical constitutive parameters obtained from rigorous experiments into the conceptual design stage of digital architectures or advanced packaging, this research holds significant industrial implications. Designers can directly utilize these highly accurate mesoscopic mechanical databases, combined with computational geometry-driven topology optimization algorithms, to customize the spatial interweaving paths of fibers and local layup thicknesses for the specific shapes and vulnerable points of packaging products. This not only fundamentally achieves a highly integrated customization of "material - structure - performance", but also promotes the deep integration of advanced numerical simulations with actual manufacturing processes. The optimized process configuration can be easily transferred to packaging structures of different geometries, dimensions and load-bearing requirements by updating the design constraints in the computational optimization framework. The winding and weaving platform is programmable, and can be adjusted the winding paths and process parameters as required according to the specific structure. For bigger or load-bearing packaging, the optimization framework can decide suitable combinations of heating temperature, winding tension, roller pressure and winding speed which can ensure the integrity of the packaging structure and guarantee the manufacturing efficiency. This adaptiveness feature further strengthens the applicability of the proposed approach to a variety of products for sustainable packaging. The proposed winding and weaving process also shows great potential for packaging production on a large scale, while maintaining sustainability. The programmable control system and optimized process parameters can be easily adopted for continuous manufacturing systems, to

enhance production efficiency and process consistency. The computational optimization tool allows for quick parameter variation with various packaging geometries and production specifications without compromising mechanical performance. Therefore, the manufacturing scheme of straw fiber/PLA composite packaging proposed in this paper is a practical way for mass production of biodegradable packaging materials in industry, which has high productivity and sustainability.

5.4 Qualitative Life Cycle and Sustainability Analysis

From a qualitative life cycle and sustainability approach, the proposed straw fiber/PLA composite material has an environmental benefit when compared to traditional petroleum-derived packaging materials, through the employment of straw waste from agriculture and biodegradable materials. In the recent LCA of PLA-coated cellulose paper straws, there have been positive results regarding its environmental sustainability along with better biodegradability and end-of-life properties, thus favoring the sustainable nature of bio-degradable packaging [36]. Likewise, the recent research work on PLA/rice straw bio composites has revealed that the use of agricultural straw as a reinforcing component would enhance resource recovery and circular economy aspects of biodegradable packaging [37]. The NSGA-II optimization technique has minimized the specific energy requirement from 90.4 kJ/kg to 89.5 kJ/kg, signifying improved energy efficiency. As opposed to traditional plastic packages, the suggested composite is anticipated to help in lowering carbon emissions through reduced dependency on fossil fuels and increased use of renewable biomass from agriculture. Moreover, the biodegradability of the material gives it positive end-of-life properties, thus ensuring reduced environmental impact when disposed off properly. In sum, these results show that the suggested composite is a sustainable material for eco-friendly packaging applications.

5.5 Modeling Assumptions and Study Limitations

The proposed manufacturing framework consists of three steps: micromechanical analysis, resin impregnation analysis based on Darcy model, and multi-objective optimization, which can be used to assess the mechanical properties of straw-fiber composite packaging under laboratory conditions. The material behavior was modeled during the computational analysis with the chosen constitutive assumptions, in order to get a consistent relationship between the fiber architecture, the resin infiltration characteristics and the structural response. The developed framework can serve as a reliable foundation for optimizing the process in the investigated manufacturing conditions and can be adapted to the natural properties of straw fibers when forming composites. Consequently, the reported outcomes represent the performance of the proposed methodology under the adopted modeling framework and support subsequent validation across broader manufacturing environments.

6. Conclusions

The study proposed a coupled optimization method of the automated three-axis winding and weaving straw-fiber/PLA composites by integrating mesoscopic material prediction, BBD, RSM, ANOVA and NSGA-II. Four process parameters, such as winding speed, winding tension, roller pressure and heating temperature, were systematically tested by applying 29 BBD experimental configurations. The properties of tensile strength, porosity, and specific energy consumption were considered as the primary performance responses. The relationship between process parameters and responses were established using RS and ANOVA and Pareto-optimal parameter combinations were identified using NSGA-II to maximize tensile strength and minimize porosity and energy consumption. The optimal conditions were then experimental tested, verifying the applicability of the proposed framework to enhance the performance of the composite manufacturing process. The following conclusions of great theoretical and engineering value were drawn:

- Revealed the narrow survival process window effect of natural fibers: The physical experiments and nonlinear mathematical models in this study clearly pointed out that due to the thermal instability of hemicellulose and lignin in the straw, the system has a strict “rebound threshold”.

- Verified the outstanding efficacy of the MDO framework in resolving multi-objective conflicts in materials engineering: Facing the three irreconcilable conflicting goals of improving material strength, enhancing density, and suppressing manufacturing energy consumption, the NSGA-II successfully derived a Pareto-optimal process configuration scheme that balances performance and cost. The verification experiments conducted based on the parameters provided by this algorithm (temperature 198.5 °C, tension 51.2 N, pressure 2.7 MPa, speed 95.4 mm/s) showed that the real tensile strength jumped to 71.8 MPa, the porosity was controlled at an extremely low 1.54%, and the actual equipment energy consumption remained at 89.5 kJ/kg, with the errors of all predicted indicators being lower than 6.2%, demonstrating extremely high theoretical.

References

[1] Rahman MA, Mojumdar S, Rahman SA, Marimuthu K. Plastic pollutions in the ocean: Their sources, causes, effects and control measures. Journal of Biological Studies. 2023;6(1):37-52. https://doi.org/10.62400/jbs.v6i1.7755

[2] Srivastava V, Singh S, Das D. Enhancing packaging sustainability with natural fiber reinforced biocomposites: An outlook into the future. E3S Web of Conferences. 2023;436:08016. https://doi.org/10.1051/e3sconf/202343608016

[3] Akhil UV, Radhika N, Saleh B, Aravind Krishna S, Noble N, Rajeshkumar L. A comprehensive review on plant-based natural fiber reinforced polymer composites: Fabrication, properties, and applications. Polymer Composites. 2023;44(5):2598-2633. https://doi.org/10.1002/pc.27274

[4] Xu F, Xu W, Xu C, Wang J, Tang H. Optimising rice straw bale quality through vibration-assisted compression. Agriculture. 2025;15(19):2094. https://doi.org/10.3390/agriculture15192094

[5] Zhang Y, Zhu QJ, Gao S, Liu S, Li LH, Chen HT. Optimization of technological parameters of straw fiber-based plant fiber seedling pot raw materials. Applied Sciences. 2021;11(15):7152. https://doi.org/10.3390/app11157152

[6] Karbuz P, Dogu M, Ozbek B. Manufacturing of hexagonal cross-section thermoplastic matrix composite parts with automatic filament winding system. Journal of Manufacturing Processes. 2024;129:62-76. https://doi.org/10.1016/j.jmapro.2024.08.051

[7] Kilani A, Fapohunda C, Adeleke O, Metiboba C. Evaluating the effects of agricultural wastes on concrete and composite mechanical properties. Research on Engineering Structures and Materials. 2022;8(2):307-336. https://doi.org/10.17515/resm2021.339st0912

[8] Mo Y, Ye S, Qaiser Z, Johnson S. Structural and winding sequence optimization of coreless filament wound composite lattice structures. International Journal of Advanced Manufacturing Technology. 2023;127(9):4903-4914. https://doi.org/10.1007/s00170-023-11761-y

[9] Mindermann P, Müllner R, Dieringer E, Ocker C, Klink R, Merkel M, et al. Design of fiber-composite/metal-hybrid structures made by multi-stage coreless filament winding. Applied Sciences. 2022;12(5):2296. https://doi.org/10.3390/app12052296

[10] Mishra DK, Singh BR, Kumar S, Sharma VK, Singh N. Design and optimization of agro-residue fiber-reinforced composite panels for sustainable grain storage. Fibers and Polymers. 2025;26(11):5023-5038. https://doi.org/10.1007/s12221-025-01114-9

[11] Ming X, Li Q, Feng J, Jiang W. Analysis and optimization of process parameters of the degradable fiber mulch paper made from pineapple leaf and rice straw by response surface method. BioResources. 2021;16(2):3454-3472. https://doi.org/10.15376/biores.16.2.3454-3468

[12] Mastouri A, Efhamisisi D, Tarmian A, Boukherroub R, Lexa M, Karami E, et al. Sustainable superhydrophobic and self-cleaning wood via wax within Epoxy/PDMS nano-composite coatings: Durability related to surface morphology. Progress in Organic Coatings. 2024;186:107951. https://doi.org/10.1016/j.porgcoat.2023.107951

[13] Geng H, Cao X, Zu L, Pan H, Zhang G, Zhang Q, et al. The effects of laser-assisted winding process parameters on the tensile properties of carbon fiber/polyphenylene sulfide composites. Materials. 2024;17(18):4664. https://doi.org/10.3390/ma17184664

[14] Borwankar P, Kapania RK, Inoyama D, Stoumbos T. Multidisciplinary design analysis and optimization of space vehicle structures. In: AIAA SciTech 2024 Forum. Reston (VA): American Institute of Aeronautics and Astronautics; 2024:2898. https://doi.org/10.2514/6.2024-2898

[15] Mosi G. Characterization and modeling of mechanical properties of additively manufactured coconut fiber-reinforced polypropylene composites. Advances in Materials Physics and Chemistry. 2025;15.

[16] Liu B, Zhang Z, Huang X, Zhang J, Cai Y, Liu X, et al. Effect of straw characterization on the mechanical behavior of compacted straw-reinforced soils. Buildings. 2025;15(9):1543. https://doi.org/10.3390/buildings15091543

[17] Zhu Q, Wang X, Xu X, Gao S, Liu S, Chen H, et al. Optimization of manufacturing parameters and experimental study of rice straw fiber-based plant fiber seedling pots. Agronomy. 2023;13(7):1782. https://doi.org/10.3390/agronomy13071782
[18] Gil Pérez M, Zechmeister C, Kannenberg F, Mindermann P, Balangé L, Guo Y, et al. Computational co-design framework for coreless wound fibre-polymer composite structures. Journal of Computational Design and Engineering. 2022;9(2):310-329. https://doi.org/10.1093/jcde/qwab081
[19] Doersam A, Larrea Murillo L, Jones C, Tsigkou O. Developing scalable woven textile-based scaffolds for tubular tissues with core-sheath nanofibre yarns and tuneable weave architectures. Frontiers in Bioengineering and Biotechnology. 2025;13:1655852. https://doi.org/10.3389/fbioe.2025.1655852
[20] Meshram SD, Gupta S, Kulthe M, et al. The role of additive manufacturing in the study of carbon fiber-reinforced polymer composite. Polymer Bulletin. 2024;81:15469-15511. https://doi.org/10.1007/s00289-024-05476-7
[21] Senk V. Mechanics of plant fiber-reinforced composite materials: From micro-meso modeling to interactive frameworks for material-informed design in early planning phases [dissertation]. Vienna: Technische Universität Wien; 2025.
[22] Phunpeng V, Boransan W, Horpibulsuk S. Comprehensive analysis of in-plane tensile characteristics of hybrid composite using finite element method. Journal of Engineering Research. 2025;13(2):1294-1306. https://doi.org/10.1016/j.jer.2023.11.008
[23] Memon SI, Memon AW, Memon US, Ali N. Assessment of the impact of different weave geometries on the crimp factor of woven preforms made from high-performance carbon filaments. Mehran University Research Journal of Engineering and Technology. 2025;44(2):182-187. https://doi.org/10.22581/muet1982.3383
[24] Mei F, Li B, Xu Z, Li X, Zhu X. Discrete element modeling of straw bale: An innovative approach to simulate the compression mechanics of fiber-based materials. Computers and Electronics in Agriculture. 2025;231:110002. https://doi.org/10.1016/j.compag.2025.110002
[25] Deng B, Shi Y, Yu T, Kang C, Zhao P. Multi-response parameter interval sensitivity and optimization for the composite tape winding process. Materials. 2018;11(2):220. https://doi.org/10.3390/ma11020220
[26] Zhai Z, Du Y, Wang X. Optimization of process parameters for carbon fiber reinforced polyamide 6 composites fabricated by self-resistance electric heating technology. Polymers. 2023;15(8):1914. https://doi.org/10.3390/polym15081914
[27] Szpisják-Gulyás N, Al-Tayawi AN, Horváth ZH, László Z, Kertész S, Hodúr CJA. Methods for experimental design, central composite design and the Box-Behnken design to optimise operational parameters: A review. Acta Alimentaria. 2023;52(4):521-537. https://doi.org/10.1556/066.2023.00235
[28] Ghadge R, Ghorpade R, Joshi S. Multi-disciplinary design optimization of composite structures: A review. Composite Structures. 2022;280:114875. https://doi.org/10.1016/j.compstruct.2021.114875
[29] Malashin I, Tynchenko V, Gantimurov A, Nelyub V, Borodulin A. A multi-objective optimization of neural networks for predicting the physical properties of textile polymer composite materials. Polymers. 2024;16(12):1752. https://doi.org/10.3390/polym16121752
[30] D'Orazio F, Cottini F, Spazzini F, Furlan V, Giberti H. A novel and flexible path planning algorithm for robotic filament winding of non-axisymmetric tubular structures. Composite Structures. 2025;373:119647. https://doi.org/10.1016/j.compstruct.2025.119647
[31] Sun Z, Duan Y, An H, Wang X, Liang S, Li N. Research progress and application of natural fiber composites. Journal of Natural Fibers. 2023;20(2). https://doi.org/10.1080/15440478.2023.2206591
[32] Dhar D, Jain A. Improved micromechanical prediction of short fibre reinforced composites using differential Mori-Tanaka homogenization. Mechanics of Materials. 2023;185:104768. https://doi.org/10.1016/j.mechmat.2023.104768
[33] Huang D, Wang W, Tang X, Zhu P, Zhao X. A novel semi-empirical analytical method for stiffness prediction of unidirectional discontinuous-fiber composites. Composites Science and Technology. 2025;262:111087. https://doi.org/10.1016/j.compscitech.2025.111087
[34] Rossa AJ, Bozó DC, Mindermann P, Gresser GT, Schuenemann F. Leveraging regionally sourced natural fibers for coreless filament winding in sustainable construction. Clean Circular Bioeconomy. 2025;100199. https://doi.org/10.1016/j.clcb.2025.100199
[35] Luo W, Xu S, Luo T, et al. Carbon emissions and economic cost of different collection, storage, and transportation models for crop straw off-field utilization. Waste and Biomass Valorization. 2024;15:2989-3001. https://doi.org/10.1007/s12649-023-02370-7
[36] Xie Y, Ji Z, Abdalkarim SYH, Huang H, Yunusov KE, Yu HY. Investigating interface adhesion of PLA-coated cellulose paper straws: Degradation, plant growth effects, and life cycle assessment. Journal of Hazardous Materials. 2024;480:136101. https://doi.org/10.1016/j.jhazmat.2024.136101
[37] Kampeerapappun P, O-Charoen N, Dhamvithee P, Jansri E. Biocomposite Based on Polylactic Acid and Rice Straw for Food Packaging Products. Polymers. 2024;16(8):1038. https://doi.org/10.3390/polym16081038